50

ELECTRICAL PHENOMENA AT INTERFACES

Fundamentals, Measurements, and Applications

Second Edition, Revised and Expanded

edited by
Hiroyuki Ohshima
Science University of Tokyo
Shinjuku-ku, Japan

Kunio Furusawa
University of Tsukuba
Ibaraki, Japan

MARCEL DEKKER, INC. NEW YORK · BASEL · HONG KONG

ISBN: 0-8247-9039-1

This book is printed on acid-free paper.

Headquarters
Marcel Dekker, Inc.
270 Madison Avenue, New York, NY 10016
tel: 212-696-9000; fax: 212-685-4540

Eastern Hemisphere Distribution
Marcel Dekker AG
Hutgasse 4, Postfach 812, CH-4001 Basel, Switzerland
tel: 44-61-261-8482; fax: 44-61-261-8896

World Wide Web
http://www.dekker.com

The publisher offers discounts on this book when ordered in bulk quantities. For more information, write to Special Sales/Professional Marketing at the headquarters address above.

Current printing (last digit):
10 9 8 7 6 5 4 3 2 1

PRINTED IN THE UNITED STATES OF AMERICA

28

Electrostatic and Electrokinetic Properties of Micelles

Toyoko Imae
Nagoya University, Nagoya, Japan

I. INTRODUCTION

The investigation of electrostatic and electrokinetic properties is important to evaluate the stabilization of dispersed colloidal particles, including surfactant micelles, in aqueous media [1]. The electrical surface structure of micelles is characterized by electrostatic potentials at the micellar surface and the Stern layer surface. Such surfaces are related to the degree of ionization and the electrical double layer of micelles, which are changed by the adsorption and/or binding of small ions. The electrostatic properties were examined by potentiometric titration and electrical conductivity, and the degree of ionization of micelles and their fractional counterion binding were calculated [2–4].

The zeta potential at the sliding plane or the immobile layer surface of micelles is concerned with electrophoresis, an electrokinetic phenomenon. The zeta potential is sometimes approximated to be the potential at the Stern layer surface, although Stigter [5] evaluated the Stern potential as being higher than the zeta potential on the basis of a structural model of the micellar surface. The electrophoretic mobility of micelles was measured by a micelle tagging method [6–8], its modification [9], and a Schlieren electrophoretic method [2,10–12]. The mobilities of ionic and weak electrolyte micelles were evaluated and compared under various conditions with respect to counterion species, added salt species, salt concentration, surfactant concentration, temperature, and pH. The measurement of the electrophoretic mobility of small colloidal particles like spherical micelles was made easier by the development of an electrophoretic light scattering instrument [13]. Some investigations using such an instrument have been reported [14–18]. In the present work, the electrokinetic properties of micelles are reviewed in relation to their electrostatic properties.

II. IONIC MICELLES

A. Ionic Micelles with Inorganic Counterions

Ionic surfactants like sodium alkyl sulfates, alkylamine hydrohalides, and alkyltrimethylammonium halides form spherical micelles. Spherical micelles sometimes change in structure to become rodlike in certain conditions such as high surfactant and salt concentrations. Then the association structure of the ionic micelles is related to their electrostatic and electrokinetic properties [19].

A micelle tagging technique based on the preferential solubility of water-insoluble dyes in the micelles was applied by Hoyer and coworkers [6,7] to determine the electrophoretic mobilities of sodium dodecyl sulfate (SDS) micelles. The charge on the SDS micelles was obtained at its critical micelle concentration (cmc).

Hoyer and Greenfield [8] investigated the electrophoretic mobilities of aliphatic amine hydrochloride micelles by the same method. The mobilities decreased with increasing surfactant concentration and with decreasing temperature. Moreover, the mobilities at the cmc were more dependent on the ionic strength of the solution than on the alkyl chain length of the monomer ions.

The charge on micelles was evaluated by Wasik and Hubbard [20] by applying the equations of Prins and Hermans and Princen and Mysels to static light scattering data. It was indicated that the nature and concentration of the gegenions (counterions) determined the charge of alkyltrimethylammonium micelles, whereas the nature and concentration of simple cations (co-ions) of the added salts had little or no effect.

The Stern layer potentials were estimated by Emerson and Holtzer [21] from numerical solutions to the nonlinearized Poisson–Boltzmann equation, assuming a sphere with smeared charge and using available data of the micellar radius and aggregation number. The Stern layer potentials, which were computed for SDS and dodecyltrimethylammonium halide micelles, decreased with concentration of added salt, consistent with results on mobilities obtained by Hoyer and Greenfield [8]. The nature of the counterions affected the electrostatic potential as well as the mobility reported by Wasik and Hubbard [20].

Mobilities of SDS micelles were obtained from moving boundary examination in a Tiselius-type Schlieren electrophoretic apparatus [12]. The measurement was also carried out with an electrophoretic light scattering spectrometer [15]. The mobilities were in good agreement between the two examinations.

Tokiwa and Ohki [2,11] reported Schlieren electrophoretic results of sodium dodecylpolyoxyethylene sulfate micelles in the presence of inorganic electrolytes and of organic electrolytes such as alkylammonium chlorides and sodium alkylcarboxylates with short alkyl chains with fewer than six carbons. The surface charge density and the effective charge numbers were obtained from the zeta potential. They elucidated that the electrophoretic mobilities and zeta potentials were influenced by the number of oxyethylene units and considerably by the valence of cations (counterions) but only slightly by the valence of anions (co-ions), as expected. The effect of the type of inorganic electrolytes on the zeta potential is similar in tendency to the effect to be expected from the Gouy–Chapman equation for spherical colloidal particles.

Recently, electrophoretic mobilities U of hexadecyltrimethylammonium bromide ($C_{16}TABr$) micelles were measured by Imae and Kakitani [22] at various surfactant concentrations. The surface charge density σ and the fractional binding of small ions β per surfactant were calculated by using Henry's equation

$$U = \frac{\sigma A m}{f}(1 + \kappa R_i)\frac{X_1(\kappa R)}{1 + \kappa(R + R_i)} \tag{1}$$

for the electrophoretic mobility of rigid spherical macro-ions [23] and a relation of

$$\sigma = e(1 - \beta)/A \tag{2}$$

where A is the surface area per surfactant, m is the micellar aggregation number, and f is the frictional coefficient. κ is the Debye–Hückel parameter, R is the radius of the rigid spherical particle, and R_i is the effective radius of the bound ion. $X_1(\kappa R)$ is a Henry's function, and e is the elementary electric charge. Parameter values of $m = 137$, $R = 2.98$ nm, and $R_{\mathrm{Br}^-} = 0.21$ nm were used. The electrophoretic mobilities increase slightly with increasing C_{16}TABr concentration C in aqueous 0.1 M NaBr solutions at 35°C, as seen in Table 1, resulting from a slight increase in the surface charge density and a slight decrease in the fractional binding of Br^-. The electrical shielding effect of 0.1 M NaBr is less for solutions of high C_{16}TABr concentrations. This results in less counterion binding and higher surface charge density. Although opposite results were reported by Hoyer and Greenfield [8], as described above, the reason for the opposite effect cannot yet be stated.

The ionization degree of C_nTABr micelles was evaluated by Zana [3] using a specific ion electrode and electrical conductivity. A decrease in the degree of ionization upon increasing alkyl chain length was shown. The degree of ionization (0.14 in water at 25°C) of C_{16}TABr micelles reported by him is close to the value (0.1–0.16 in water at 35°C) calculated from the fractional binding of Br^- in Table 1 [22]. The electrophoretic mobility measurement of C_{16}TABr micelles in an aqueous NaBr solution was carried out by Cuccovia et al. [24] according to the procedure described by Hoyer et al. [6]. The ionization degree (0.20 in 25 mM NaBr at 30°C) calculated is slightly higher than the values in water given above.

B. Ionic Micelles with Organic Counterions

When certain kinds of aromatic counterions are replaced with simple inorganic counterions as described in the previous section, the behavior of cationic micelles in solution changes remarkably [25–31]. The characteristic spinnability phenomenon

Table 1 Electrophoretic Mobility, Surface Charge Density, and Fractional Binding of Small Ions per Unit Surfactant for C_{16}TABr Micelles in 0.1 M NaBr Solutions at 35°C[a]

C (mM)	U ($\times 10^{-4}$ cm^2 V^{-1} s^{-1})	σ (cm^{-2})	β
20	1.39	0.017	0.90
40	1.73	0.021	0.88
60	2.09	0.026	0.85
80	2.13	0.026	0.85
100	2.27	0.028	0.84

[a] cmc = 0.2 mg/cm^3.

and the viscoelasticity in strong correlation with it were reported for aqueous solutions of alkyltrimethylammonium and alkyltrimethylpyridinium salicylates [25,26,28,29,31]. The solution behavior results from the formation of rodlike micelles that build the three-dimensional pseudo network by entangling and contacting each other [30,31]. The characteristic rheological behavior is not observed in aqueous solutions of entangled rodlike micelles of cationic surfactants with halide counterions [31]. Then salicylate counterions play an important role in solution behavior as well as in micellar size. Salicylate ions must be located near the micellar surface, because they exhibit specific adsorption and penetration ability [27]. Thus it is necessary to elucidate the electrical structure of micelles and the interaction forces between micelles.

Imae and Kohsaka [16,17] investigated the size and electrophoretic mobility of tetradecyl- and hexadecyltrimethylammonium salicylate (C_{14}TASal; C_{16}TASal) micelles in aqueous media by using light scattering. Whereas short rodlike micelles were formed in aqueous solutions without sodium salicylate (NaSal), the length of the rodlike micelles increased with an increase in NaSal concentration and reached a maximum in 0.1 M NaSal. Further addition of NaSal diminished the micellar size, as confirmed from the result that micelles in 1 M NaSal were spherical. The ionic strength dependence of micellar size and shape was consistent with the change in spinnability and viscoelastic behavior [28,29]. The examination of electrophoretic mobility indicated the conversion of sign from positive to negative through neutral at about 0.1 M NaSal, as seen in Fig. 1, indicating the reversal of the net surface charge of the micelles. This shows that specific adsorption and penetration of salicylate ions dominate the micellar size and solution behavior. Then the role of salicylate ions must be focused on. Schematic models of surface potentials for micelles

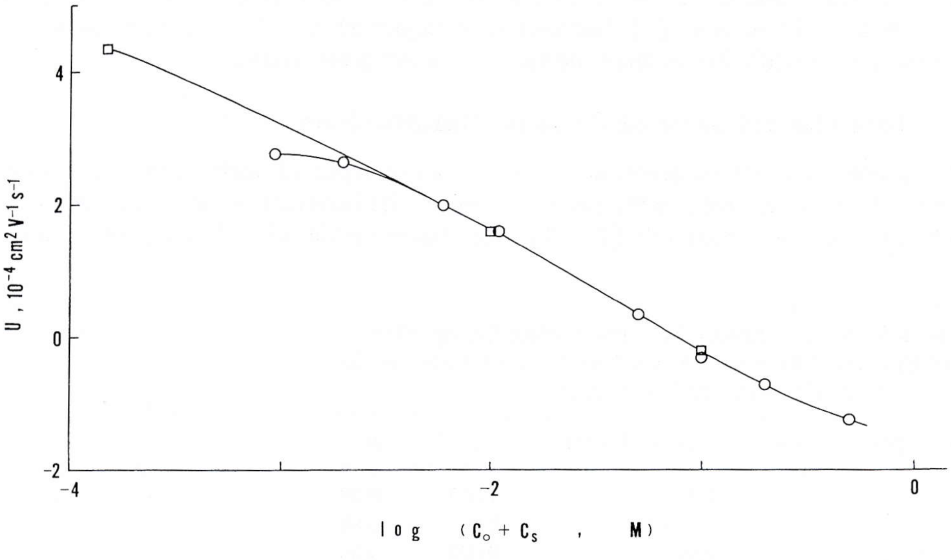

Figure 1 Electrophoretic mobilities of C_nTASal micelles in aqueous NaSal solutions as a function of ionic strength at 25°C. (○) C_{14}TASal (8 mg/cm^3); (□) C_{16}TASal (0.55 mg/cm^3). C_0 and C_S are critical micelle concentration and NaSal concentration, respectively. (From Ref. 17.)

within different NaSal concentration regions were proposed along with models of the molecular arrangement on the micellar surface, as drawn in Fig. 2.

The formation of a 1 : 1 complex between alkyltrimethylammonium ion and salicylate ion was postulated by Shikata et al. [32] and supported by Bachofer and Turbitt [33] and Nemoto and Kuwahara [34]. However, Cassidy and Warr [35] cast some doubt on this idea. They determined surface potentials of mixtures of C_{14}TABr and NaSal in water by the titration of a micelle-bound indicator, 4-heptadecyl-7-hydroxycoumarin. They found a strong binding of salicylate ion that is effective at lowering the surface potential of the micelles. However, even at a 100-fold excess of salicylate over C_{14}TABr, no reversal in the sign of the electrostatic potentials at the micellar surface was observed, as seen in Fig. 3. On the other hand, the zeta potentials calculated from electrophoretic mobility by using the Smoluchowski equation [1] were lower than the electrostatic potentials at the micellar surface. Therefore, their results do not support the existence of a stoichiometric 1 : 1 complex proposed by Shikata et al. [32]. The model proposed by Cassidy and Warr [35] corresponds to a continuous variability in the adsorption sites, which are the exterior surface of the micelle to bind salicylate and the hydrophobic core of the micelle to intercalate salicylate.

A new instrument for measurement and analysis of surface interactions and forces (MASIF) was developed by Parker [36]. The instrument was used by Kato et al. [37] for the force measurement of C_{16}TASal films adsorbed on glass beads from aqueous NaSal solutions. The force F normalized by the beads' radius R is plotted in Fig. 4 as a function of separation for aqueous solutions of various NaSal concen-

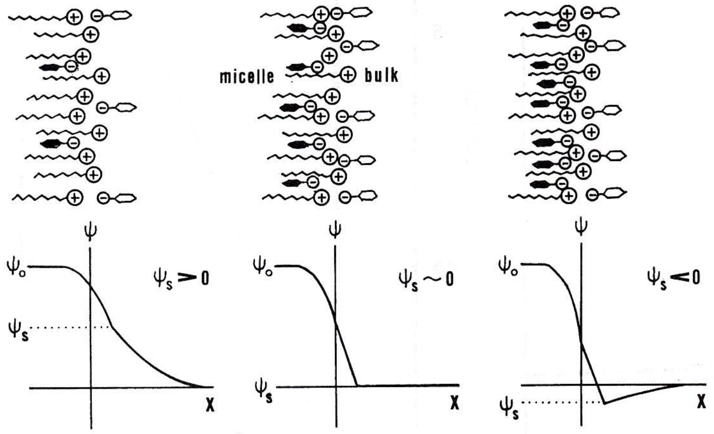

(1) (2) (3)

Figure 2 Schematic representation of the molecular arrangement and electrostatic potential ψ on C_nTABr micellar surface at NaSal concentrations of (1) ∼0 M; (2) ∼0.1 M; (3) ∼1 M. ⊕∼, surfactant ion; ⊖—⬡, salicylate ion adsorbed on micellar surface; ⊖—⬢, salicylate ion that has penetrated into a micelle. ψ_0 and ψ_S are the electrostatic potentials at the micellar surface and the Stern layer surface, respectively. X denotes the distance from the micellar surface. (From Ref. 17.)

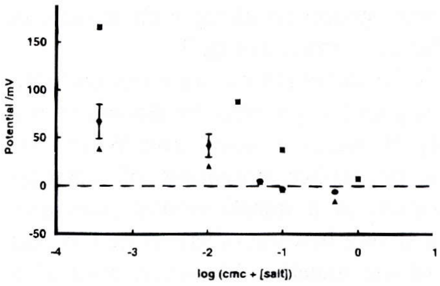

Figure 3 The electrostatic potential at the micellar surface (■) and the zeta potential (●) as a function of total ionic strength for aqueous NaSal solutions of $C_{14}TABr$ at a surfactant concentration of 25 mM. (▲) Zeta potential calculated from electrophoretic mobilites for NaSal solutions of $C_{14}TASal$ at a surfactant concentration of 25 mM. (From Ref. 35.)

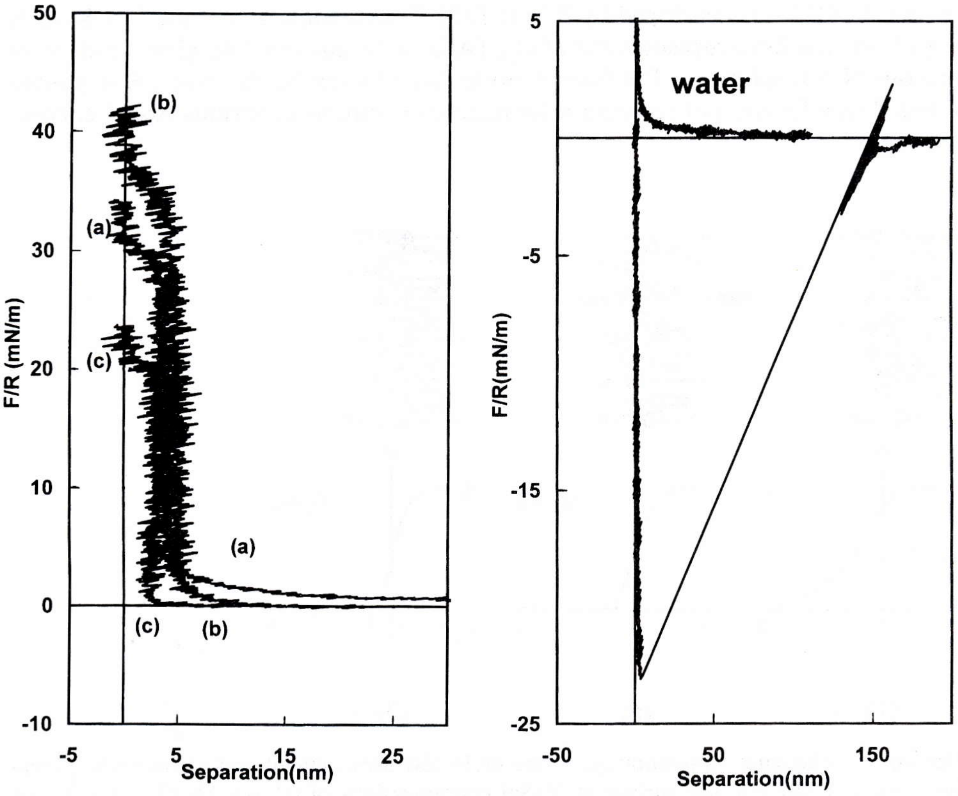

Figure 4 Force vs. separation curves for aqueous NaSal solutions of $C_{16}TASal$ at a surfactant concentration of 0.15 mM. Left: The inward process with NaSal concentrations of (a) 0 M; (b) 0.1 M; (c) 1 M. Right: The outward process for an aqueous solution of $C_{16}TASal$ without NaSal. A force vs. separation curve for water is also included. (From Ref. 37.)

trations at a surfactant concentration of 0.15 mM. While the electrostatic repulsive interaction occurs at longer separation for a solution without NaSal, it decreases with the addition of NaSal. This is consistent with the diminution of the electrostatic potential and zeta potential described above.

The characteristic profile common for all solutions is the step-in phenomenon. The step-in distance is 3–5 nm. The distance corresponds to separations of about two layers. The step-in occurs at 20–40 mN/m, depending on NaSal concentration. Interesting results were obtained on the outward process where two surfaces in contact are pulled apart. As shown in Fig. 4, strong adhesion occurred for all solutions examined. The interlocking decreases with increasing NaSal concentration. This tendency agrees with that of the electrostatic potential and the zeta potential. The interlocking is stronger than that of hexadecyltrimethylammonium chloride [38]. This implies a strong interaction between salicylates in the adsorbed state or between adsorbed salicylate and micelle.

The interaction between cationic surfactant and NaSal was investigated on surfaces of silica particles. Favoriti et al. [39] reported that below the cmc hexadecylpyridinium chlorides adsorbed at a silica/water interface and formed a double layer structure. Salicylate ions coadsorb owing to strong interaction between the surfactant head group and the aromatic anion. Above the cmc, the salicylate ions are distributed among adsorbed surfactant aggregates, free micelles, and water. It was also suggested that the ion partition coefficient expressed as the ratio of bound-to-free salicylate concentrations depended on the solution pH above the silica isoelectric point. At low pH values, salicylate ions form complexes with the cationic head groups of surfactant in the inner layer facing the silica surface. At high pH values, salicylate ions are repelled from the inner layer by the high negative surface charge density on the silica particles. On the other hand, the surfactant in the outer layer facing the bulk of the solution complexes the aromatic anions at any pH. This configuration is closer to that of free micelles.

III. WEAK ELECTROLYTE MICELLES

Since the weak electrolyte surfactants alkyldimethylamine oxide (C_nDAO) and oleyldimethylamine oxide (ODAO) are protonated at acid pH to convert into *N*-hydroxyammonium ions [11,40], the solution behavior depends on pH [40–45]. The lower critical solution temperature of the consolute boundary in the liquid–liquid phase separation is lowest at medium protonation [40]. Micellar growth and the micellar structural transition from sphere to rod are remarkable at medium protonation [41]. The micellar contour length between pseudo-network meshes, which are formed by entangled rodlike micelles in the semidilute regions, is greater at degrees of protonation of 0.2–0.5 [44]. Simultaneously, the rheological behavior increases. The more marked characteristics are the strong effect of external interference in light scattering originating from the intermicellar interaction [42] and the iridescent phenomenon explained by the interference of light arising from the Bragg reflection between multilamellar layers [45]. These characteristics appear in aqueous solutions of C_nDAO and ODAO without salt at neutral pH and disappear with addition of salt or acid. It was suggested that the nonideal characteristics depending on pH of aqueous solutions of C_nDAO and ODAO were related to the hydration and protonation of surfactants in micelles at neutral and acid pH, respectively, and the hydrogen bonding between amine oxide residue and *N*-hydroxyammonium ion in micelles at medium degrees of protonation [42]. Moreover, the intermolecular and intermicellar interactions such as electrostatic repulsion, hydrogen bonding, and hydration that occurs in concert with the stabilization of C_nDAO and ODAO micelles were affected by the addition of salt.

The electrophoretic mobilities of protonated $C_{12}DAO$ micelles were measured with the moving boundary method by Tokiwa and Ohki [11]. The mobilities in 0.1 M NaCl depended on pH. The zeta potentials of the electrical double layer were calculated from the electrophoretic mobilities and compared with the electrostatic potentials of micellar surfaces that were evaluated by means of potentiometric titration. The electrostatic potentials and zeta potentials decreased with decreasing degree of protonation, as expected. Furthermore, the zeta potential was always lower than the electrostatic potential, suggesting the specific adsorption of Cl^- on protonated micellar surfaces.

Imae and coworkers [18,46] performed electrophoretic light scattering measurements for aqueous NaCl solutions of C_nDAO ($n = 12,14$) and ODAO. As seen in Fig. 5, the electrophoretic mobilities for 0.1 and 0.2 M NaCl solutions of C_nDAO changed from negative to positive as the degree of protonation α increased. The observed values are slightly lower than those obtained by Tokiwa and Ohki [11]. Moreover, Tokiwa and Ohki do not report negative mobility at zero degree of protonation. It can be assumed that they did not notice the opposite movement of the boundary at that condition. On the other hand, three kinds of electrophoretic mobilities were observed for 0.05 M NaCl solutions of C_nDAO, depending on the degree of protonation, as seen in Figs. 5 and 6, although for 0.03 M NaCl solutions of ODAO the positive mobilities increased continuously with degree of protonation

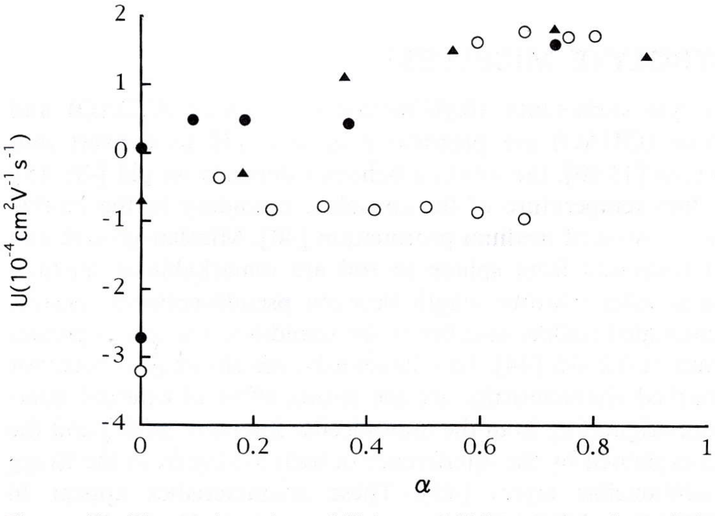

Figure 5 Electrophoretic mobilities at 25°C as a function of degree of protonation for aqueous NaCl solutions of $C_{12}DAO$ at a surfactant concentration of 10 mg/cm^3. NaCl concentrations: (○) 0.05 M; (●) 0.1 M; (▲) 0.2 M. (From Ref. 46.)

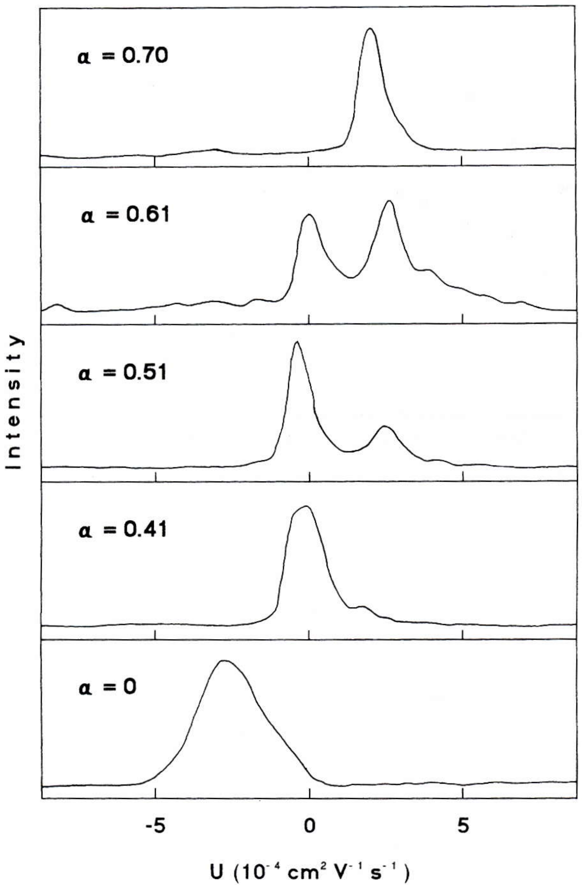

Figure 6 Electrophoretic light scattering power spectra at 25°C for 50 mM NaCl solutions of C_{14}DAO at a surfactant concentration of 5 mg/cm^3. (From Ref. 18.).

[18]. The fractional binding of small ions and Cl^-, that is, β and β_{Cl^-}, were evaluated from the electrophoretic mobility on the basis of the equation

$$\sigma = e(\alpha - \beta)/A \tag{3}$$

and potentiometric titration conducted with a specific ion electrode [46]. Both values were consistent at all degrees of protonation for 0.1 M NaCl solutions of C_{12}DAO, as illustrated in Fig. 7. However, such consistency was obtained only at higher degrees of protonation for 0.05 M NaCl solutions of C_{12}DAO.

Electrophoretic mobilities are related to the electrostatic potentials of micelles, which are affected by the protonation of a micelle and the counterion binding. Then the experimental results are explained in relation to the variation of the electrostatic potentials. The negative electrophoretic mobility at $\alpha = 0$ can be explained by the adsorption of chloride ions on micellar surfaces. The adsorption is maintained by the interaction between the polarized amine oxide and the hydrated water on chloride ions. The hydration adsorption of chloride ions disappears with the protonation of surfactant. Instead, in 0.1 M NaCl solutions of C_nDAO, chloride ions bind

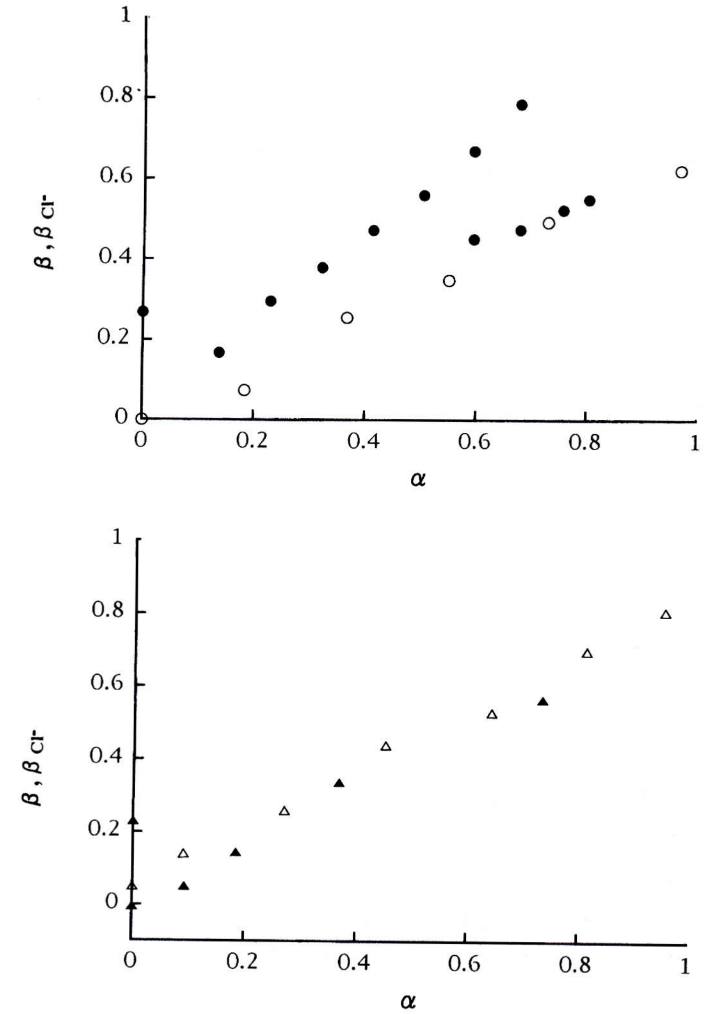

Figure 7 Fractional bindings of small ions and Cl^- on $C_{12}DAO$ micelles at a surfactant concentration of 10 mg/cm^3 in aqueous NaCl solutions at 25°C. Upper: In 0.05 M NaCl. (●) β; (○) β_{Cl^-}. Lower: In 0.1 M NaCl. (▲) β; (△) β_{Cl^-}. (From Ref. 46.)

electrostatically on micelles with keeping certain fraction. In 0.05 M NaCl solutions, although this kind of micellar species exists at $\alpha > 0.5$, micellar species at $\alpha = 0.1$–0.7 are different (see Fig. 8). Excess chloride ions adsorb on micelles beside electrostatically bound chloride ions. The adsorption forces may include the interaction through the hydrated water as well as the adsorption of chloride ions at $\alpha = 0$. The excess chloride ions may exist between the Stern layer surface and the sliding plane and exchange easily with free ions. In the present situation, however, the reason that the third micellar species coexists with the second species in 0.05 M NaCl solutions is not yet clear.

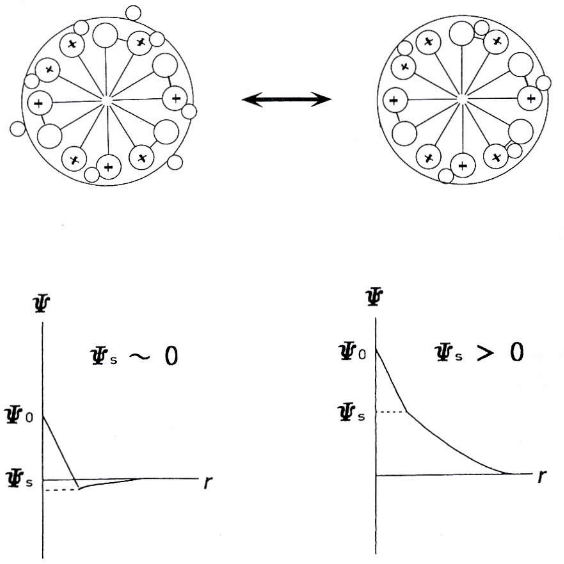

Figure 8 Schematic representation of counterion binding on C_nDAO micelles and electrostatic potential at their surfaces in solutions at medium degrees of protonation. (From Ref. 46.)

IV. MIXED MICELLES

When different kinds of surfactants are mixed, the solution properties behave ideally or nonideally, depending on the combination. The nonideal behavior may result from the intramicellar interaction between heterogeneous surfactants and the competitive binding of small ions. These are related to the electrostatic and electrokinetic potentials of mixed micelles. Tokiwa [2] reported zeta potentials of mixed micelles of sodium dodecylpolyoxyethylene sulfate (SDPS) and dodecylpolyoxyethylene ether (DPOE). The zeta potentials decreased with increasing DPOE/SDPS ratio. However, the decrease displayed an upward curvature, that is, a deviation from ideal behavior.

Rathman and Scamehorn [4] reported potentiometric titration using specific ion electrodes on micellar solutions composed of mixtures of anionic/nonionic, cationic/nonionic, anionic/anionic, and cationic/cationic surfactants consisting of nonionic surfactants such as alkylpolyethoxylates, alkylphosphine oxides, alkylamine oxides, and alkylsulfoxides and ionic surfactants such as hexadecyltrimethylammonium chloride, alkylpyridinium chloride, SDS, and sodium octylbenzenesulfonate. The fractional counterion bindings changed ideally for ionic/ionic surfactants but nonideally for ionic/nonionic surfactants.

On the other hand, Kameyama and Takagi [15] reported the electrophoretic mobilities of octaethylene glycol dodecyl ether micelles mixed with SDS by using electrophoretic light scattering photometry. The mobilities increased with the addition of SDS for molar ratios less than 0.3. The linear increase in the mobility in this condition indicates the stoichiometric increase of surface charge upon the addition of SDS.

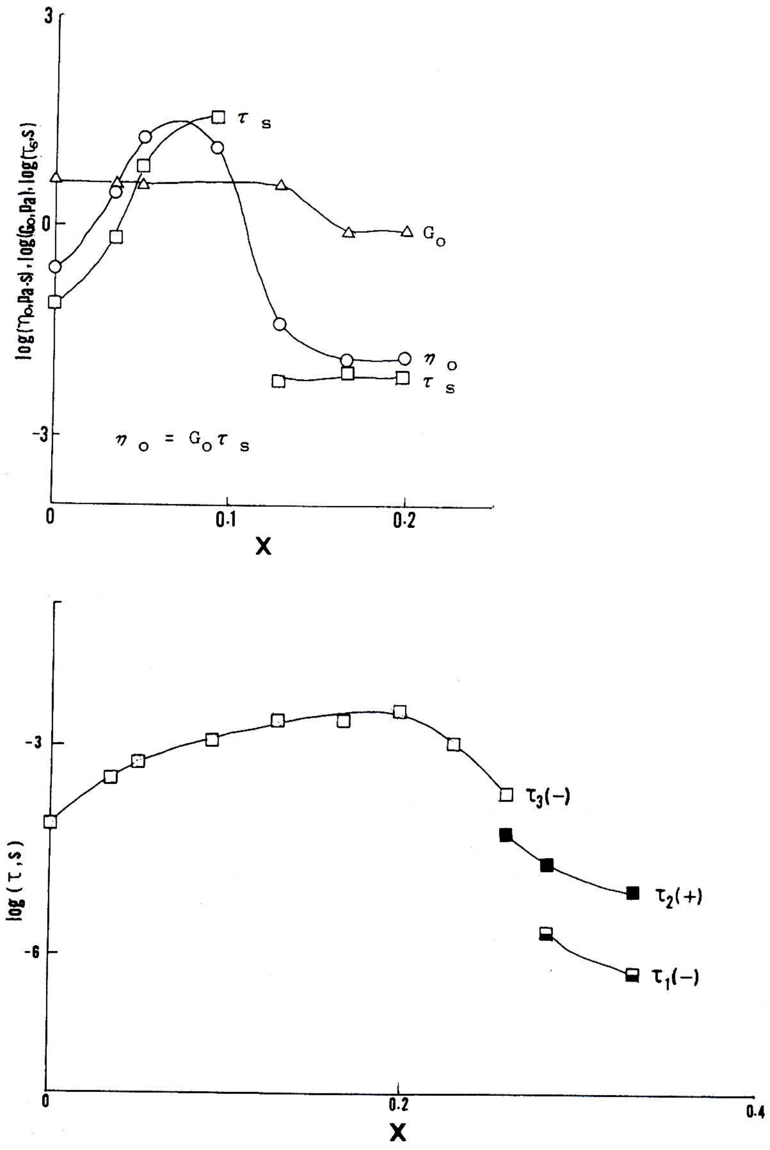

Figure 9 Zero shear viscosities η_0, plateau moduli G_0, and relaxation times τ as a function of mixing fraction for aqueous solutions of C_{16}DAO/SDS mixtures at 35°C. A total surfactant concentration is 50 mM. τ_S and τ_i ($i = 1, 2, 3$ were obtained from rheological and electrical birefringence measurements, respectively. (+) and (−) denote the sign of the relaxation time. (From Ref. 52.)

The surface charge density of C_nDAO micelles can be altered by adding ionic surfactants such as C_nTABr and SDS, instead of HCl, to aqueous solutions of C_nDAO. Then the behavior of the mixed solutions depends on the type of ionic surfactant. While the mixture of C_nDAO and C_nTABr behaves ideally, the effect of SDS on C_nDAO micelles is nonideal; the solution pH, the cmc, the micellar aggregation number, and the partial molar volume deviate from ideal behavior, but not the heat capacity [47–50], although the rheological behavior is nonideal for both C_nDAO/C_nTAB and C_nDAO/SDS mixtures [47,51,52].

The transient electrical birefringence for mixed solutions of $C_{16}DAO$ and SDS at a total surfactant concentration of 80 mM at 35°C displays different patterns with changing mixing molar fraction X ($= [SDS]/([C_{12}DAO] + [SDS])$), indicating the existence of three relaxation processes with relaxation time τ_i, as seen in Fig. 9 [52]. The additional relaxation time τ_s is observed from the viscoelastic measurement and plotted in Fig. 9, where other rheological data are also included. The relaxation times and the rheological data are maximized at $X = 0.1$–0.2. Similar results have already been reported for mixed solutions of $C_{14}DAO$ and SDS by Hofmann et al. [51]. It was suggested that the nonideal behavior of C_nDAO/SDS complex in solutions was due to the ion pairing of the self-protonated amine oxide with sulfate [53]. The solution behavior mentioned above is related to the electrostatic interaction, which is controlled by the mixing fraction of ionic surfactant in C_nDAO micelles and by the existence of small ions on micelles and in bulk solution. Thus, the investigation of the electrical surface structure of mixed micelles becomes important.

Electrokinetic properties of mixed solutions of $C_{12}DAO$ and SDS were investigated by electrophoretic light scattering and the potentiometric titration of Na^+ [54]. The electrophoretic mobilities of the micelles and their surface charge densities, calculated according to Eq. (1), were always negative at all mixing fractions, as seen in Fig. 10. This indicates the specific adsorption of Cl^-, as well as Na^+, on the micelles. The fractional binding of small ions, β, is calculated by inserting the known value of the surface charge density on the relation

$$\sigma = e(\beta - 1)/A \tag{4}$$

On the other hand, the fractional binding of Na^+, β_{Na^+}, is calculated from Na^+ titration. Then the adsorption of Cl^-, β_{Cl^-}, is determined as the difference of β and

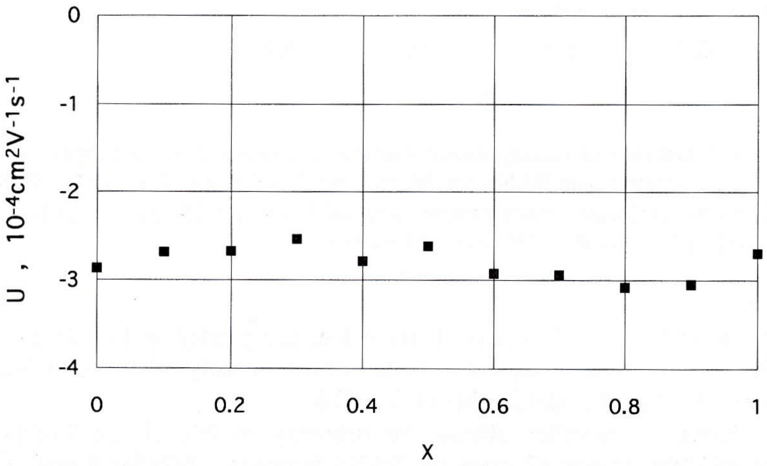

Figure 10 Electrophoretic mobilities as a function of mixing molar fraction for 50 mM NaCl solutions of C_{12} DAO/SDS mixture at 25°C. The total surfactant concentration is 80 mM.

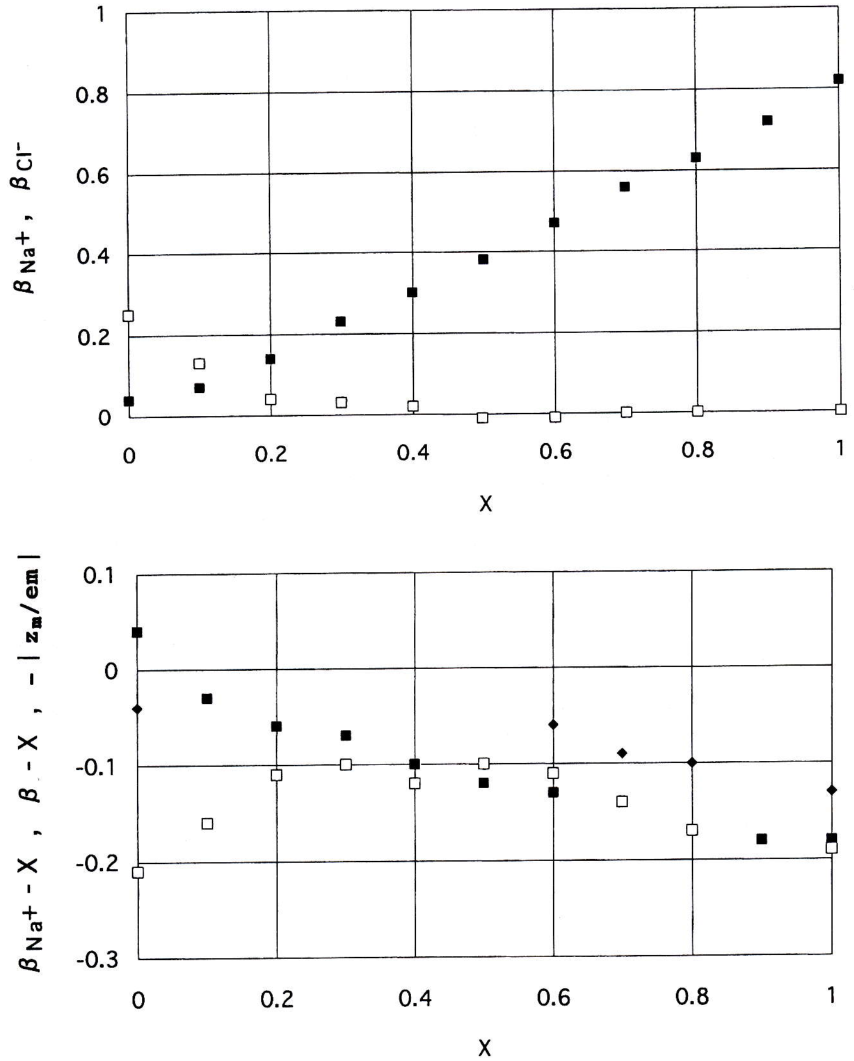

Figure 11 Data, as a function of mixing molar fraction, evaluated from electrophoretic mobility, potentiometric titration, and SANS for 50 mM NaCl solutions of C_{12}DAO/SDS mixture at 25°C. The total surfactant concentration is 80 mM. Upper: (■) β_{Na^+} ; (□) β_{Cl^-}. Lower: (■) $\beta_{Na^+} - X$; (□) $\beta - X$; (◆) $-|Z_m/em|$. (From Ref. 54.)

β_{Na^+} values or $\beta - X$ and $\beta_{Na^+} - X$ values. Their values are plotted in Fig. 11 as a function of mixing molar fraction. β_{Na^+} increases almost linearly with increasing mixing fraction up to 1, while β_{Cl^-} diminishes at $X > 0.4$.

The surface charge on micelles affects the intensity profile of small-angle neutron scattering (SANS). Figure 12 gives the SANS intensities $I(Q)$ for 0 and 50 mM NaCl solutions of C_{12}DAO/SDS mixtures at different mixing fractions [53]. The interparticle interference effect resulting from interparticle interaction such as electrostatic repulsion was observed except for 50 mM NaCl solutions at medium

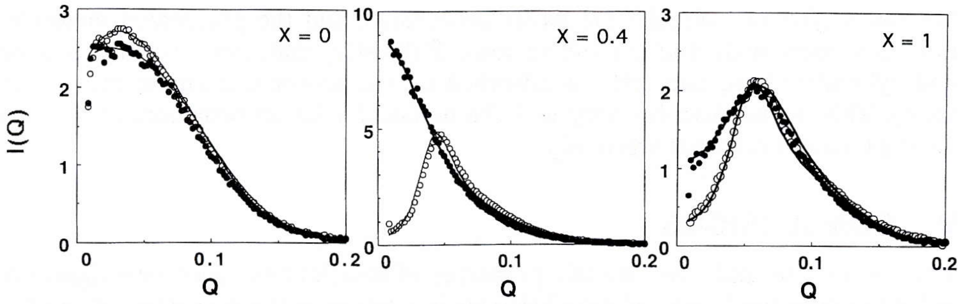

Figure 12 SANS data for 0 and 50 mM NaCl solutions of C_{12}DAO/SDS mixtures at different mixing molar fractions. The total surfactant concentration is 80 mM. NaCl concentrations: (○) 0 M; (●) 50 mM. The solid lines are the calculated curves. Q is the magnitude of the scattering vector. (From Ref. 53.)

mixing fractions. The SANS intensities were analyzed by using a rescaled mean spherical approximation for the interparticle structure factor [50]. In the analysis, the electrostatic repulsive interaction was taken into account. The evaluated average electric charge number per surfactant monomer, $-|z_m/em|$, is included in Fig. 11, where z_m is the electric charge of the macro-ion. This value must be equivalent to $\beta - X$. However, the former is systematically lower than the latter. This can be interpreted as the difference between the definition of Stern layer thickness detected by the electrophoretic method and the SANS. The schematic models of electrical surface structure for mixed micelles of C_{12}DAO and SDS in 50 mM NaCl are illustrated in Fig. 13 [54]. The surface structure at X ≈ 0 was discussed in the foregoing section. Amine oxide head groups attract chloride ions through hydrogen bonding mediated by water. At $X \approx 1$, counterions diffuse partly into bulk solution as usual. However, a different kind of electrical surface structure appears at a medium molar

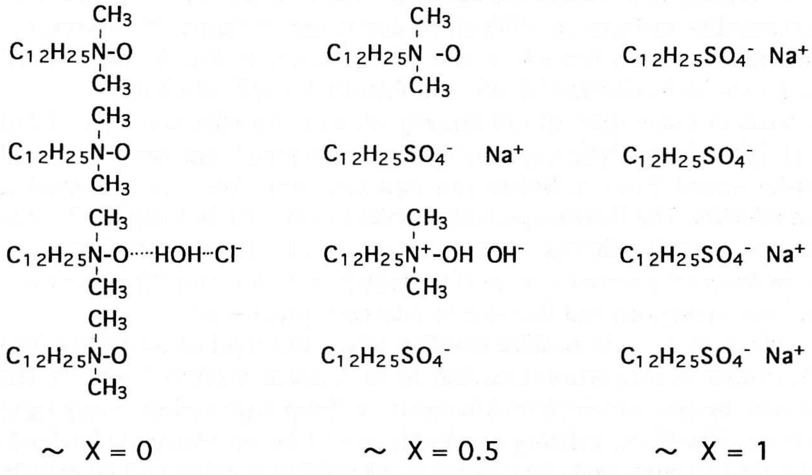

Figure 13 Schematic representation of molecular species in mixed micelles at different mixing molar fractions. (From Ref. 54.)

fraction. $C_{12}DAO$ molecules are partly protonated, and the protonated molecules form ion pairs with dodecyl sulfate ions. Following that, Na^+ is adsorbed on dodecyl sulfate ions, and OH^- is adsorbed on the protonated amine oxide head group. This model describes very well the nonideal solution behaviors at medium mixing fractions reported previously.

V. CONCLUSIONS

The electrostatic and electrokinetic properties of micelles have been investigated in order to understand their solution behavior in relation to the properties of micellar surfaces. Although the electrostatic potential and ion binding at the micellar surface could be evaluated from the potentiometric titration, it was previously difficult to examine the Stern layer potential and the zeta potential. The development of the electrophoretic light scattering technique opened the way to study the electrokinetic properties of colloidal particles, especially surfactant micellar systems. However, the reports for micelles are very few, even now. One reason is the small size of micelles and the weak light scattering intensities of micellar solutions. These problems will be solved with improved measurement techniques and a powerful light source.

The second problem is to determine a plausible model of the micellar surface structure and develop an adequate expression of the corresponding theory. Stigter and Mysels [5,7] suggested that the surface of charged micelles was not smooth but rough. On the other hand, Rathman and Scamehorn [4] developed a localized adsorption model and a mobile adsorption model to describe the binding of small ions on micelles. Both models, which are based on electrostatic considerations, reproduce the binding data very well, although Rathman and Scamehorn stated that the localized adsorption model was preferred on physical grounds. They also showed that an electrostatic model could be used to predict accurately the fractional counterion binding on ionic/nonionic micelles. Their results are consistent with the concept that ionic/nonionic surfactant interactions and non-ideal properties in mixed micelles are primarily of electrostatic origin and the specific chemical interactions are of secondary importance. However, the location and the localization of counterions on micellar surfaces are difficult to determine or define. Moreover, the surface of spherical micelles is too soft to use Henry equation, Eq. (1), as assumed from the descriptions by Stigter and Mysels and Rathman and Scamehorn.

The theoretical consideration of ion binding on ionic micelles was carried out by Evans et al. [55,56]. Analytic expressions for electrostatic free energy derived from the non-linearized Poisson–Boltzmann equation were used to construct a theory of ionic micelles. The thermodynamics implicit in the ion binding model was shown to emerge naturally without resort to Stern layers. They insisted that the reconciliation of theories allowed one to discriminate between real "ion binding" due to specific ion interactions and that due to adsorption excesses.

Micelles sometimes grow to rodlike micelles, which are rigid or wormlike. The analysis of electrokinetic properties described in the present work is based on the theory for flat surfaces like Smoluchowski's equation. Such a procedure is not valid for rodlike micelles. Therefore, a theory applicable to rodlike micelles must be developed. Then the electrostatics and electrokinetics of rodlike micelles will be exactly interpreted and the electrical surface properties of charged rodlike micelles will be elucidated.

ACKNOWLEDGMENTS

I am grateful to Mr. T. Kohsaka, M. Kakitani, N. Hayashi, Y. Usami, and M. Kato for their assistance in electrophoretic light scattering, potentiometric titration, and surface force measurements.

REFERENCES

1. R. J. Hunter, *Zeta Potential in Colloid Science*, Academic, London, 1981.
2. F. Tokiwa, *J. Phys. Chem. 72*:4331 (1968); *J. Colloid Interface Sci. 28*:145 (1968); *Advn. Colloid Interface Sci. 3*:389 (1972).
3. R. Zana, *J. Colloid Interface Sci. 78*:330 (1980).
4. J. F. Rathman and J. F. Scamehorn, *J. Phys. Chem. 88*:5807 (1984); *Langmuir 3*:372 (1987).
5. D. Stigter, *J. Phys. Chem. 68*:3603 (1964).
6. H. W. Hoyer, K. J. Mysels, and D. Stigter ,*J. Phys. Chem. 58*:385 (1954).
7. D. Stigter and K. J. Mysels, *J. Phys. Chem. 59*:45 (1955).
8. H. W. Hoyer and A. Greenfield, *J. Phys. Chem. 61*:735 (1957).
9. L. Sepulveda and J. Cortes, *J. Phys. Chem. 89*:5322 (1985).
10. T. Nakagawa and H. Inoue, *Nippon Kagaku Zasshi 78*:636 (1957).
11. F. Tokiwa and K. Ohki, *Bull. Chem. Soc. Jpn. 41*: 2828 (1968); 1216 (1969).
12. T. Tokiwa and K. Aigami, *Kolloid Z. Z. Polym. 239*:687 (1970).
13. B. R. Ware and W. H. Flygare, *Chem. Phys. Lett. 12*:81 (1971); *J. Colloid Interface Sci. 39*:670 (1972).
14. T. Imae, W. Otani, and K. Oka, *J. Phys. Chem. 94*:853 (1990).
15. K. Kameyama and T. Takagi, *J. Colloid Interface Sci. 140*:517 (1990).
16. T. Imae, *J. Phys. Chem. 94*:5953 (1990).
17. T. Imae and T. Kohsaka, *J. Phys. Chem. 96*:10030 (1992).
18. T. Imae and N. Hayashi, *Langmuir 9*:3385 (1993).
19. J. N. Israelachvili, *Intermolecular and Surface Forces*, Academic, London, 1985.
20. S. P. Wasik and W. D. Hubbard, *J. Res. Nat. Bur. Stand. A Phys. Chem. 68A*:359 (1964).
21. M. F. Emerson and A. Holtzer, *J. Phys. Chem. 69*:3718 (1965); *71*:1898 (1967).
22. T. Imae and M. Kakitani, unpublished data.
23. D. H. Henry, *Proc. Roy. Soc. (Lond.) A133*:106 (1931).
24. I. M. Cuccovia, E. Feitosa, H. Chaimovich, L. Sepulveda, and W. Reed, *J. Phys. Chem. 94*:3722 (1990).
25. S. Gravsholt, *J. Colloid Interface Sci. 57*:575 (1976).
26. H. Rehage and H. Hoffmann, *Faraday Discuss. Chem. Soc. 76*:363 (1983).
27. U. Olsson, O. Soderman, and P. Guering, *J. Phys. Chem. 90*:5223 (1986).
28. T. Imae, K. Hashimoto, and S. Ikeda, *Colloid Polym. Sci. 268*:460 (1990).
29. K. Hashimoto, T. Imae, and K. Nakazawa, *Colloid Polym. Sci. 270*:249 (1992).
30. T. M. Claussen, P. K. Vinson, J. R. Minter, H. T. Davis, Y. Talmon, and W. G. Miller, *J. Phys. Chem. 96*:474 (1992).
31. T. Imae, in *Structure and Flow in Surfactant Solutions* (ACS Symp. Ser. 578) (C. A. Herb and R. K. Prud'homme, Eds.), Am. Chem. Soc., Washington, DC, 1994, p. 140.
32. T. Shikata, H. Hirata, and T. Kotaka, *Langmuir 4*: 354 (1988).
33. R. Bachofer and R. M. Turbitt, *J. Colloid Interface Sci. 135*:325 (1990).
34. N. Nemoto and M. Kuwahara, *Langmuir 9*:419 (1993).
35. M. A. Cassidy and G. G. Warr, *J. Phys. Chem. 100*:3237 (1996).
36. J. L. Parker, *Langmuir 8*:551 (1992).
37. M. Kato, T. Imae, and M. Rutland, unpublished data.
38. C. Abraham and M. W. Rutland, unpublished data.

39. P. Favoriti, M. H. Mannebach, and C. Treiner, *Langmuir 12*:4691 (1996).
40. A. Abe, T. Imae, A. Shibuya, and S. Ikeda, *J. Surf. Sci. Technol. 4*:67 (1988).
41. S. Ikeda, M. Tsunoda, and H. Maeda, *J. Colloid Interface Sci. 70*:448 (1979).
42. T. Imae and S. Ikeda, *J. Colloid Interface Sci. 98*:363 (1984); *113*:449 (1986); *Colloid Polym. Sci. 263*:756 (1985).
43. H. Zhang, P. L. Dubin, and J. I. Kaplan, *Langmuir 7*:2103 (1991).
44. T. Imae, *J. Jpn. Oil Chem. Soc. 41*:616 (1992).
45. T. Imae and T. Iwamoto, *J. Colloid Interface Sci. 152*:289 (1992).
46. T. Imae, Y. Usami, and N. Hayashi, unpublished data.
47. J. G. Weers, K. F. Rathman, and D. R. Scheuing, *Colloid Polym. Sci. 268*:832 (1990).
48. M. S. Bakshi, R. Crisantino, R. De Lisi, and S. Milioto, *J. Phys. Chem. 97*:6914 (1993).
49. N. Gorski, M. Gradzielski, and H. Hoffmann, *Langmuir 10*:2594 (1994).
50. M. Kakitani, T. Imae, and M. Furusaka, *J. Phys. Chem. 99*:16018 (1995).
51. S. Hofmann, A. Rauscher and H. Hoffmann, *Ber. Bunsenges. Phys. Chem. 95*:153 (1991).
52. T. Imae and H. Hoffmann, unpublished data.
53. T. Imae, *Colloids Surf. A*: *Physicochem. Eng. Aspects 109*:291 (1996).
54. T. Imae and M. Kakitani, *Colloid Polym. Sci. 274*:1170 (1996).
55. D. F. Evans and B. W. Ninham, *J. Phys. Chem. 87*:5025 (1983).
56. D. F. Evans, D. J. Mitchell, and B. W. Ninham, *J. Phys. Chem. 88*:6344 (1984).